N95- 23819

STATUS OF LDEF RADIATION MODELING

John W. Watts
ES84, NASA/Marshall Space Flight Center
AL 35812
Phone: 205/544-7696, Fax: 205/544-7754

T. W. Armstrong and B. L. Colborn
Science Applications International Corporation
Route 2, Prospect, TN 38477
Phone: 615/468-2603, Fax: 615/268-2676

S3-72
10P

ABSTRACT

The current status of model prediction and comparison with LDEF radiation dosimetry measurements is summarized with emphasis on major results obtained in evaluating the uncertainties of present radiation environment model. The consistency of results and conclusions obtained from model comparison with different sets of LDEF radiation data (dose, activation, fluence, LET spectra) is discussed. Examples where LDEF radiation data and modeling results can be utilized to provide improved radiation assessments for planned LEO missions (e.g., Space Station) are given.

INTRODUCTION

The return of LDEF has provided a unique opportunity to test current ionizing radiation models with a great variety of measurements. Figure 1 (ref. 1) describes the characteristics of the LDEF mission and measurements that are important for these comparisons and figure 2 (ref. 1) shows the models and programs whose outputs have been compared to the measurements of various LDEF experiments.

PROTON DOSE

There were a number of experiments (ref. 2, 3) which contained thermoluminescent dosimeters (TLD) with sufficient shielding so that the geomagnetically trapped protons contributed nearly all the accumulated dose observed. These measurements provide a good test of the Vette trapped proton model AP8MIN and AP8MAX(ref.6). Figures 3, 4, and 5 from (ref. 7) show comparisons of measurements with predictions both as ratios (Figures 3 and 5) and mission dose (Figure 4). The Figure 3 ratios suggest that the Vette models predict fluxes that are about 0.6 of the actual fluxes. Energy dependence of the ratio is not evident since the ratio is constant over a large range of effective shield thicknesses. Figure 5 shows a test of the directional model(ref. 8) against measurements. The higher observed ratios suggest that the proton scale heights used in the model are low. The comparisons are somewhat complicated by the effects of shielding geometry. Both a complex geometry model of the spacecraft and accounting of the proton directionality are required to match the trends observed in the measurements. One is not sufficient without the other.

ELECTRON DOSE

TLD measurements behind thin shields ($< 1.0g/cm^2$) provide a test of the AE8MIN and AE8MAX geomagnetically trapped electron models(ref. 9). These were a number of measurements on LDEF that meet this requirement(ref. 4, 5). In Figure 6 from (ref. 7) these measurements are compared to predicted values for a plane slab shielding geometry(ref. 10) with generally good agreement considering the difficulty of the measurements for very thin geometries. The high predictions at the thinnest shielding may reflect an excess of low energy electrons in the models or geometry effects where the detector thicknesses are comparable with the shield thickness.

PROTON ACTIVATION

The LDEF measurements of activation samples for so many location and shielding depths on a single satellite with a long-term stable attitude is unique. The ^{22}Na activation measurements of the tray clamps are little confused by geometry and the surface is well mapped by numerous samples. In Figure 7 from (ref. 11) these measurements(ref. 12, 14) are compared with the directional flux model(ref. 8, 11, 12) combined with both detailed and simple geometrical shielding models. The predictions are lower than the measurements by about the same ratios seen in the TLD versus predicted dose comparisons, again suggesting that the Vette proton flux model(ref. 6) predicts low fluxes for low orbital altitudes. The anisotrophy of the proton flux is more evident in these measurements than in any others on LDEF.

Table 1. Ratio of predicted-to-measured activity
at recovery for nickel activation samples from (ref. 11)

	Sample Location on LDEF			
Isotope	Exp. P0006	Exp. A0114	Exp. M0002	Exp. M0001
Sc-46	0.29			
Mn-54	0.62	0.34	0.73	0.33
Co-56	0.66	0.69	1.24	0.59
Co-57	0.49	0.48	0.46	0.63
Co-58	0.71	0.69	0.55	0.56
Co-60	0.84	0.49		
Average	0.60	0.54	0.74	0.53

Average for all samples: 0.60±0.15

Tables 1 and 2 from (ref. 11) show intentional sample measurements for nickel (Table 1) and vanadium (Table 2) at a variety of shielding depths. Again the measurements are higher than the model predictions with most of the ratios near those observed for dose and ^{22}Na activation. Some of the other ratios may be explained by contributions from galactic cosmic rays or uncertainties in activation cross sections used in the models. The general trend supports the conclusion from the other comparisons that the Vette flux predictions(ref. 3) are low.

Table 2. Comparison of Sc-46 activation in vanadium samples from (ref. 11)

Sample Location			Activity at Recovery (picocuries/kg)		Ratio
Exp.	Tray	Position	Measured	Calculated	Meas./Calc.
P0006	F2	trailing edge	17±1.1 (a)	7.00	0.40
			21±2.7 (b)		0.33
A0114	C9	leading edge	20±1.5 (b)	7.65	0.38
M0001	H12	space end	20±13 (b)	8.76	0.44
			22±6.8 (b)	9.50	0.44
M0002	G12	earth end	16±1.3 (b)	9.16	0.57
			16±1.4 (c)		0.58
				Average	0.46±0.16

LET SPECTRA

The long mission exposure on LDEF allowed the measurement of the Linear Energy Transfer (LET) spectra to be extended to higher LET with better statistical accuracy than has been achieved previously(ref. 15). Measurements at higher LET are significant because particles with higher LET are more likely to produce Single Event Upsets (SEU)s of microelectronic devices (an important problem for spacecraft applications). Figure 8 from (ref. 16) shows comparisons between model(ref. 17) and measured LET spectra. At high LET the measurements are significantly higher than the model. At low LET where protons are the most common particle the model results are higher. This suggest the possibility that not all the protons are being detected due to their very thin tracks. The differences at high LET are more difficult to explain, but the modeling approach ignores nuclear interactions and the produced fission fragments.

Iron nuclei fluxes are of interest because these particles have the largest charges and therefore largest LET of any particles that are fairly abundant. (elemental abundances takes a major step downward just beyond iron.) Figure 9 from (ref. 18) show LDEF measurements of the iron energy spectra. The excess over fluxes expected from galactic cosmic rays in the energy range (100-800 MeV) has been attributed to particles arriving during the large solar particle events in the fall of 1989. For iron nuclei in this energy range to arrive at the LDEF orbit through the Earth's magnetic field they must not have been completely stripped of electrons and the results suggest a charge near +12-13 similar to iron in the corona. In Figure 10 from (ref. 11, 19) the

LDEF measured Fe fluxes are used to replace the Fe fluxes used in CREME(ref. 17) for a 500 km altitude orbit at 28.5°. (The flux is not strongly dependent on altitude.) The result suggest that CREME predicts high fluxes of the low energy component of the heavier particles.

SUMMARY

The LDEF ionizing radiation measurements continue to provide a unique opportunity to test the current models of the particle environment that will not be repeated in the foreseeable future. Careful use of the models considering the details of shielding geometry and particle anisotrophy, and model assumptions are required to explain some of the trends observed in the measurements. Only with this attention to detail can we locate where the models have significant problems describing the environment or the measurements have observation difficulty.

REFERENCE

1. Armstrong, T. W.,; Colborn, B. L. and Watts, J. W.: Radiation Calculations and Comparisons with LDEF Data. First LDEF Post-Retrieval Symposium, NASA CP-3134, 1991, pp. 347-360.

2. Benton, E. V.; Frank, A. L.; Benton, E. R.; Csige, I.; Parnell, T. A. and Watts, J. W.: Radiation Exposure of LDEF: Initial Results. First LDEF Post-Retrieval Symposium, NASA CP-3134, 1991, pp. 325-338.

3. Frank, A. L.; Benton, E. V.; Armstrong, T. W. and Colborn, B. L.: Absorbed Dose and Predictions on LDEF. Second LDEF Post-Retrieval Symposium, NASA CP-3194, 1992, pp. 163-170.

4. Bourieau, J.: LDEF: Dosimetric Measurements Results (A0138-7) Experiment. Second LDEF Post-Retrieval Symposium, NASA CP-3194, 1992, pp. 157-162.

5. Blake, J. B. and Immamoto, S. S.: A Measurement of the Radiation Dose to LDEF by Passive Dosimetry. Second LDEF Post-Retrieval Symposium, NASA CP-3194, 1992, pp. 147-155.

6. Sawyer, Donald M. and Vette, James I.: AP-8 Trapped Proton Environment for Solar Maximum and Solar Minimum. National Science Data Center, Goddard Space Flight Center, NSSDC/WDC-A-R& S 76-06, 1976.

7. Armstrong, T. W. and Colborn, B. L.: Radiation Model Predictions and Validation Using LDEF Satellite Data. Second LDEF Post-Retrieval Symposium, NASA CP-3194, 1992, pp. 207-220.

8. Watts, J. W.; Parnell, T. A.; and Heckman, H. H.: Approximate Angular Distribution and Spectra for Geomagnetically Trapped Protons in Low-Earth Orbit. High Energy Radiation Background in Space, Proceedings of AIP Conference, Sanibel Island, Florida, Vol. 186, 1989, pp. 75-85.

9. Vette, J. I.: The AE8 Trapped Electron Model Environment. National Space Science Data Center, Goddard Space Flicht Center, NSSDC/WDC-A-R&S 91-24, 1991.

10. Watts, J. W.; Parnell, T. A.; Derrickson, J. H.; Armstrong, T. W.,; and Benton, E. V.: Prediction of LDEF Ionizing Radiation Environment. First LDEF Post-Retrieval Symposium. NASA CP-3134, 1991, pp. 213-224.

11. Armstrong, T. W. and Colborn, B. L.: Prediction of LDEF Induced Radioactivity and Comparison with Measurements. Third LDEF Post-Retrieval Symposium, NASA CP-3275, 1995.

12. Colborn; B. L. and Armstrong; T. W.: Development and Application of a 3-D Geometry/Mass Model for LDEF Satellite Ionizing Radiation Assessments. Second LDEF Post-Retrieval Symposium, NASA CP-3194, 1992, pp. 195-206.

13. Harmon, B. A.; Fishman, G. J.; Parnell, T. A.; and Laird, C. E.: Induced Radioactivity in LDEF Components. First LDEF Post-Retrieval Symposium, NASA CP-3134, 1991, pp. 301-312.

14. Harmon, B. A.; Fishman, G. J.; Parnell; T. A. and Laird; C. E.: Induced Activation Study of LDEF. Second LDEF Post-Retrieval Symposium, NASA CP-3194, 1992, pp. 125-136.

15. Benton, E. V.; Csige, I.; Oda, K.; Henke, R. P.; Frank, A. L.; Benton, E. R.; Frigo, L. A.; Parnell, T. A.; Watts, J. W. Jr.; and Derrickson, J. H.: LET Spectra Measurements of Charged Particles in the P0006 Experiment of LDEF. Second LDEF Post- Retrieval Symposium, NASA CP-3194, 1993.

16. Armstrong, T. W. and Colborn, B. L.: Prediction of LET Spectra Measured on LDEF. Third LDEF Post-Retrieval Symposium, NASA CP-3275, 1995.

17. Adams, J. H. Jr.: Cosmic Ray Effects on Microelectronics, Part IV, Naval Research Laboratory NRL Memorandum Report 5901, December 1986.

18. Tylka, A. J.; Adams, J. H.; Beahm, L. P.; Boberg, P. R. and Kleis, T.: Results from the HIIS Experiment on the Ionic Charge State of Solar Energetic Particles. Third LDEF Post-Retrieval Symposium, NASA CP-3275, 1995.
tion.)

19. Space Station Ionizing Radiation Emission and Susceptibility for Ionizing Radiation Environment Compatibility. SSP 30512, National Aeronautics and Space Administration, 1991.

Unique Features of LDEF Mission	*Importance to Ionizing Radiation Data Collection*	*Importance to Model/Code Validation*	*Importance to Future LEO Missions*
• Well-instrumented for ionizing radiation measurements	• Extensive radiation dosimetry: - *6 different types of dosimetry* - *multiple dosimeters of each type (≈ 200 TLD's, > 500 PNDT's, > 400 activation samples)* - *multiple dosimetry locations (in 16 different experimental trays)*	• Data sufficiently extensive and detailed to allow variety of modeling checks - e.g.: - *absorbed dose* - *proton and heavy ion fluence* - *energy spectra* - *LET spectra* - *secondary neutron fluence and spectra*	• Allows benchmarking and improvements of predictive methods for addressing ionizing radiation issues: - *dose to astronauts* *electronics upset/burnout* - *materials damage* - *radiations backgrounds to sensitive instrumentation*
• Long mission duration	• High statistical accuracy of dosimetry results	• Unprecedented data accuracy for checking model predictions of high-LET radiation from high-Z cosmic rays and nuclear recoils	• High-LET radiation component is of key importance in assessing "single-hit" phenomena: - *biological effects* - *Single-Event-Upsets of electronics*
• Fixed orientation (< 0.2° wobble during mission)	• Allows measurement of trapped proton anisotropy	• Unprecedented data for testing models of trapped proton anisotropy	• Trapped proton anisotropy important for LEO, fixed-orientation spacecraft (such as Space Station Freedom, EOS)

Figure 1. Significance of LDEF data for validation of ionizing radiation models from (ref. 1).

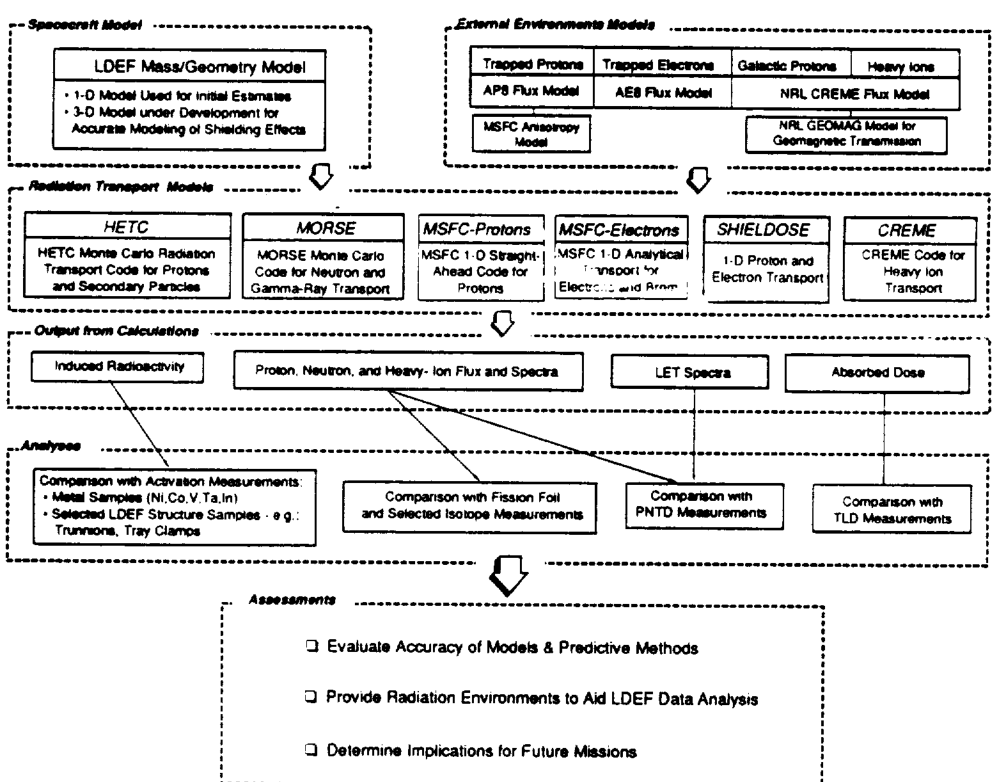

Figure 2. Overview of approach and models for LDEF ionizing radiation calculations from (ref. 1).

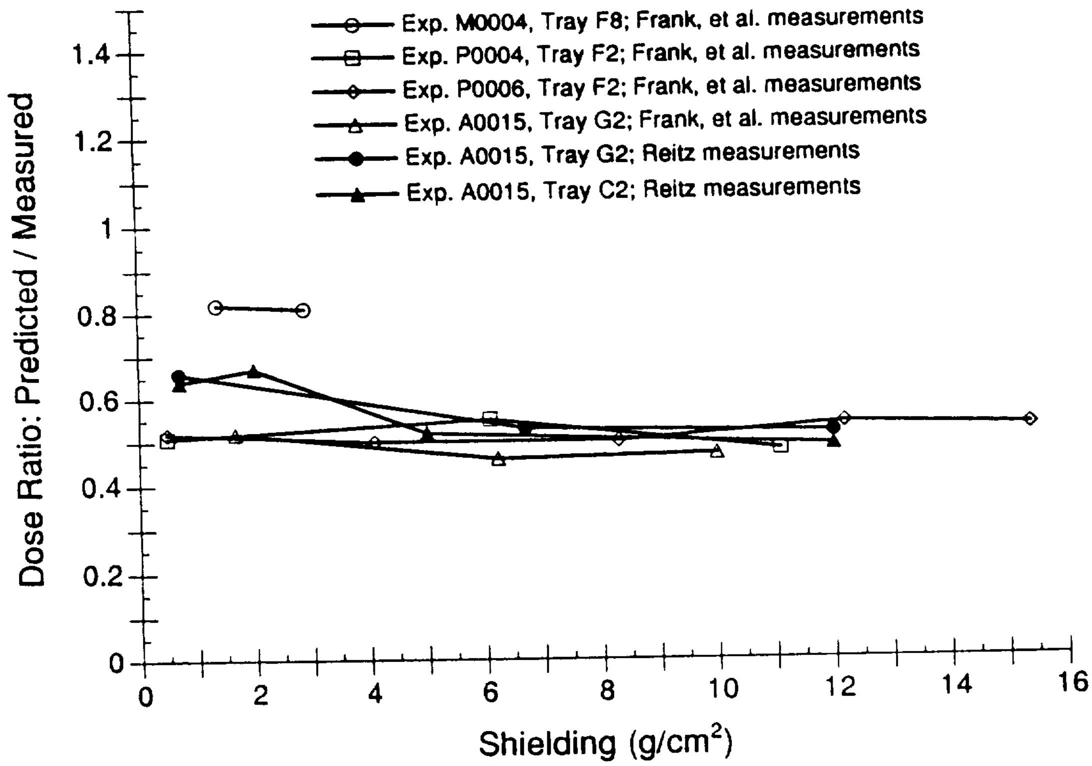

Figure 3. Ration of predicted-to-measured radiation dose (in tissue) due to trapped proton environment based on LDEF data from thermoluminescent dosimeters from (ref. 7).

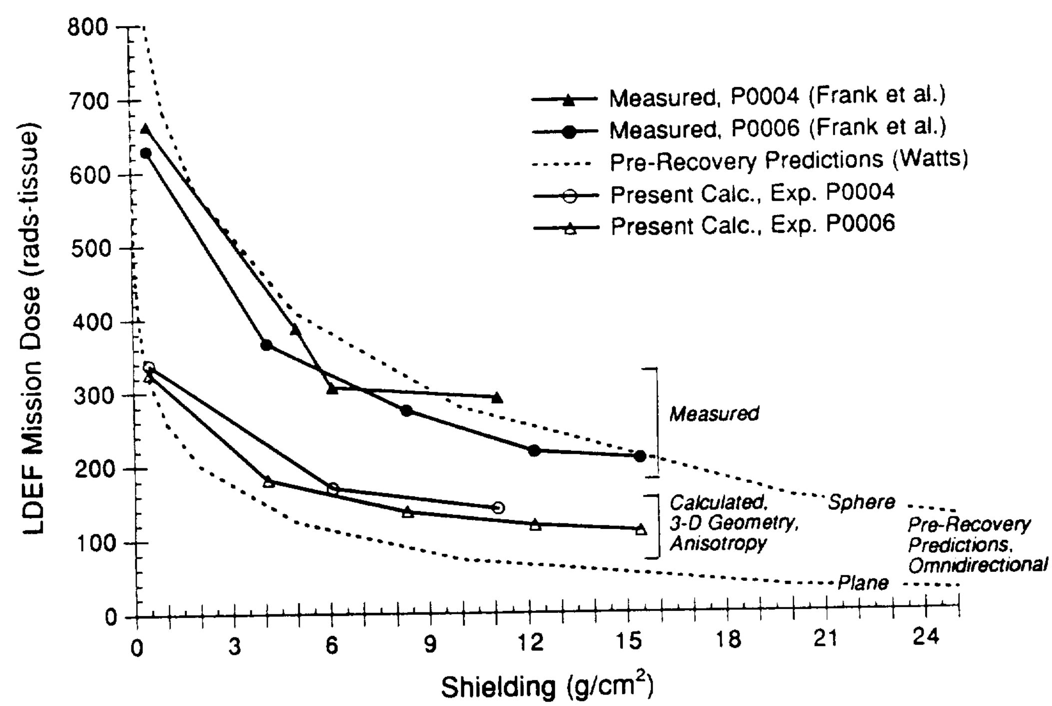

Figure 4. Influence of geometry model and environment anisotrophy on predicting LDEF dose from trapped protons from (ref. 7).

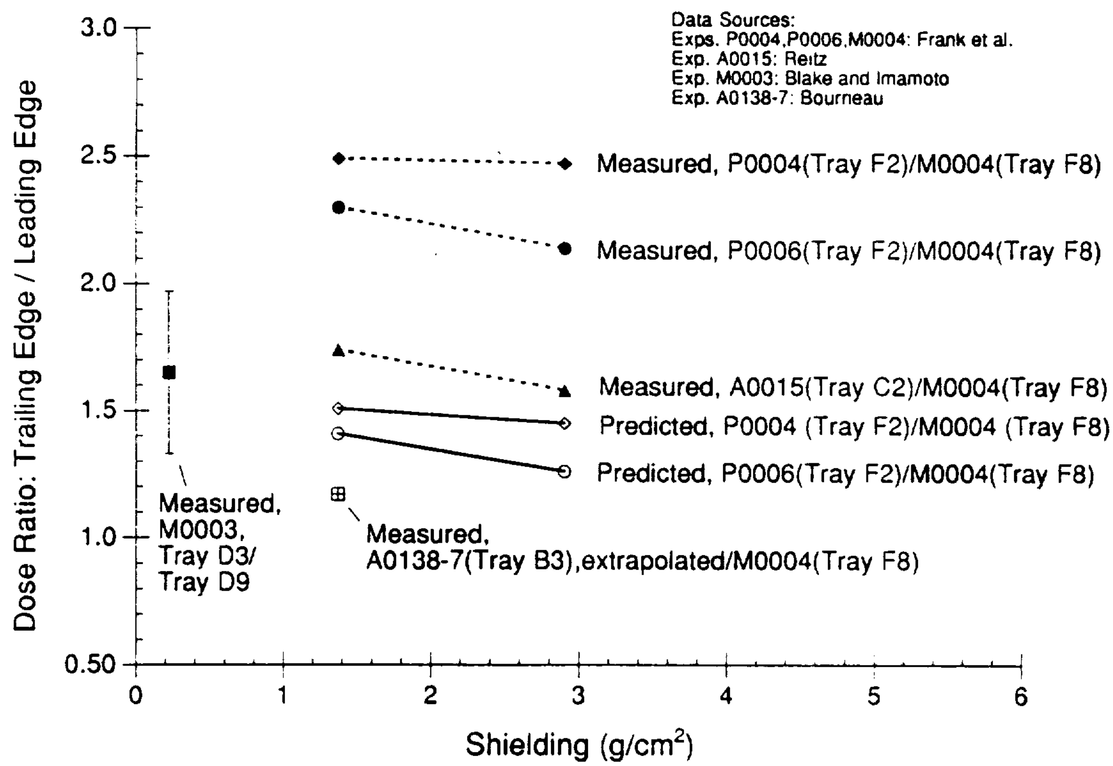

Figure 5. Radiation dose anisotrophy on LDEF due to the directionality of the trapped proton environment. Shown are predicted and measured values of the ratio for the dose on the trailing (west) side LDEF to the dose on leading (east) side from (ref. 7).

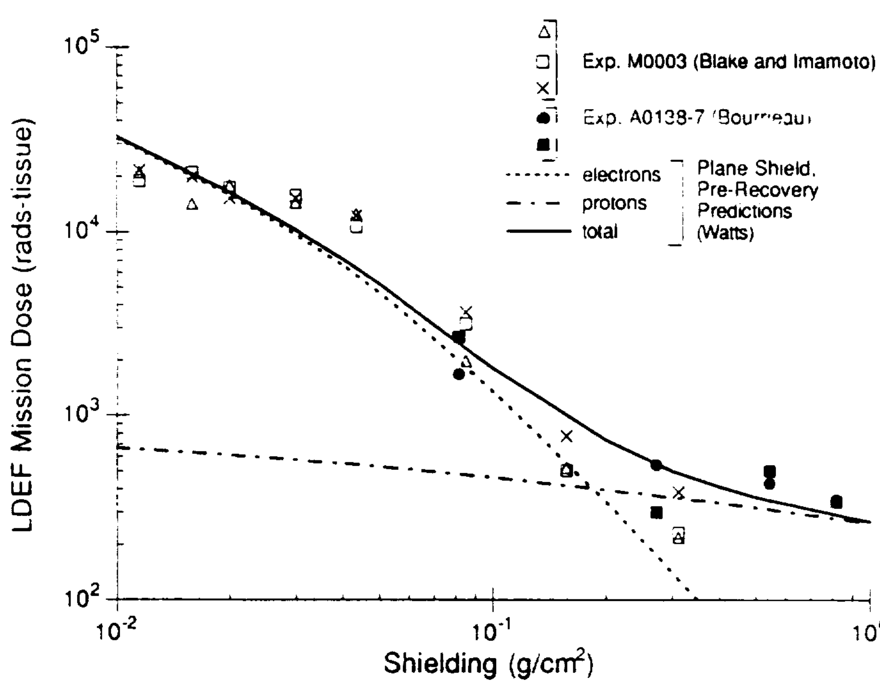

Figure 6. Comparison of measured and predicted absorbed dose for thermoluminescent dosimeters having thin shielding where the dose is due to the trapped electron environment from (ref. 7).

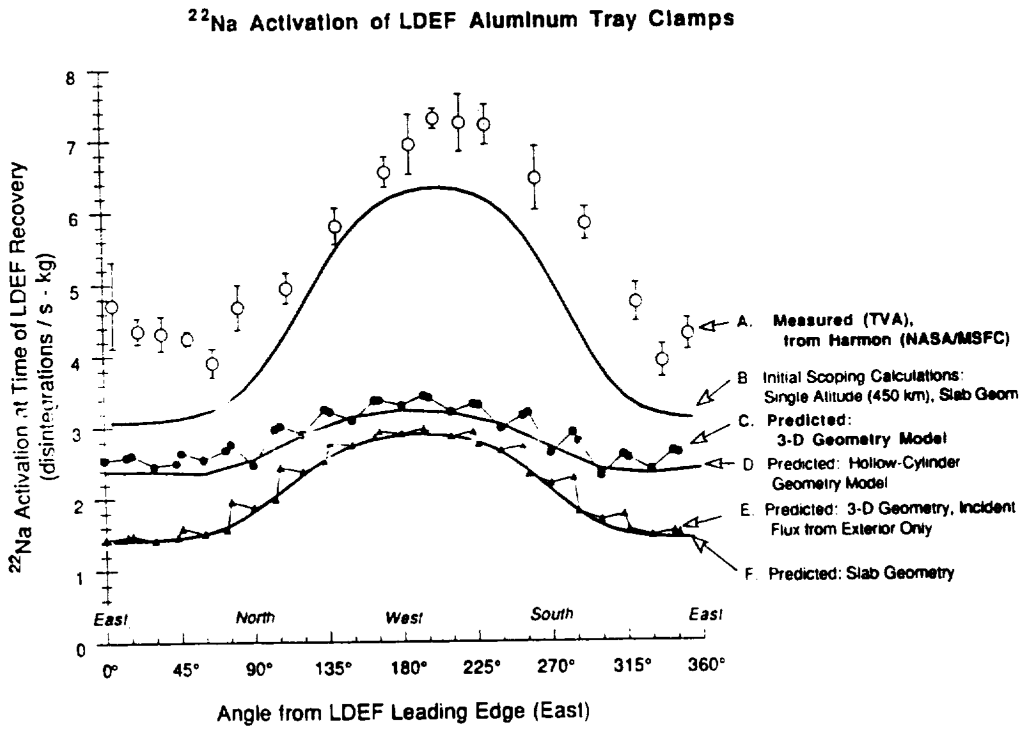

Figure 7. Preliminary comparison of predicted vs. measured effect (ref. 13, 14) of trapped proton anisotrophy in terms of ^{22}Na radioactivity induced in aluminum clamps of LDEF experiment trays from (ref. 11).

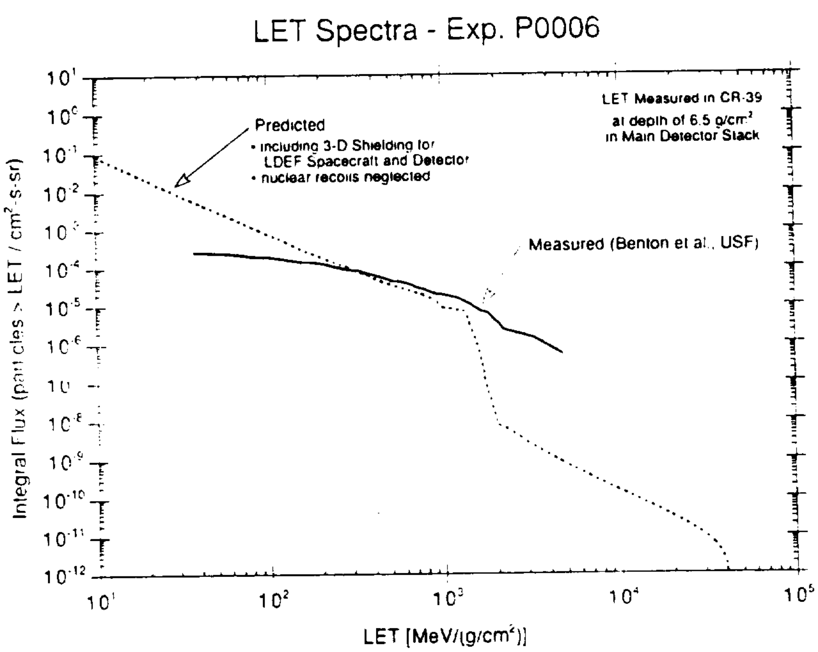

Figure 8. Comparison of LDEF predictions of Linear Energy Transfer (LET) spectra and interim results from measured spectra in experiment P0006(ref. 15). The predictions were made using the CREME code(ref. 17) and a 3-D shielding geometry from (ref.16) .

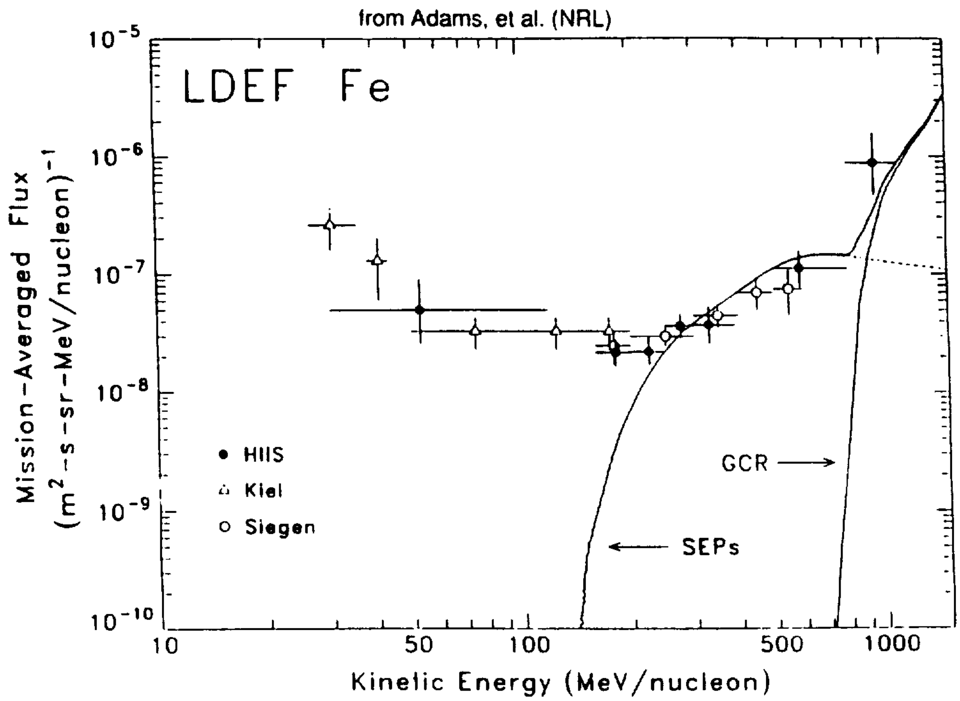

Figure 9. Measured low energy Fe spectra measured by HIIS experiment on LDEF from (ref. 18).

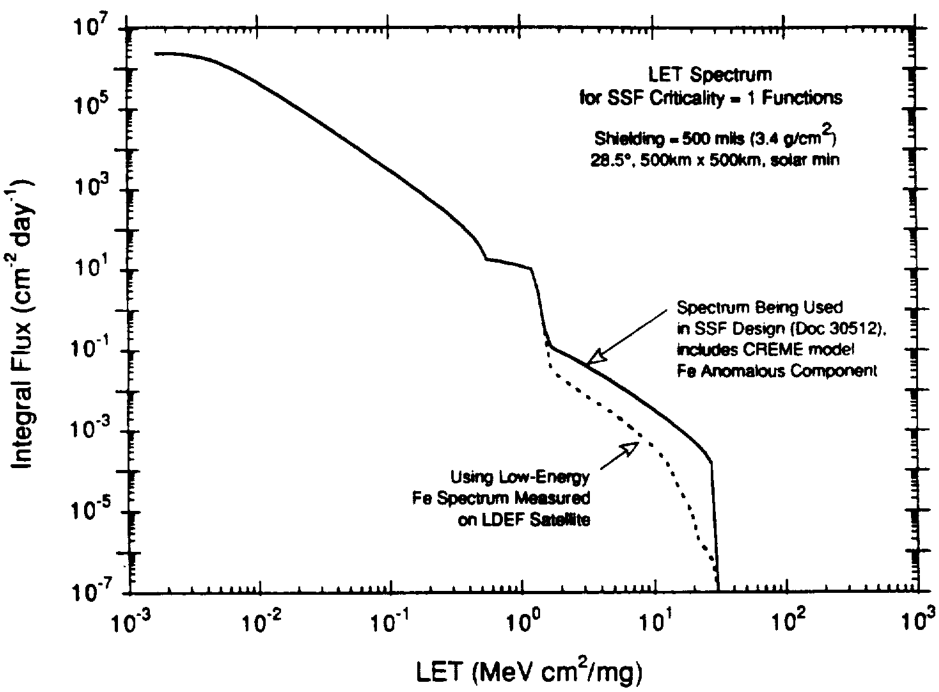

Figure 10. Comparison of Space Station Freedom Requirement document SSP 30512 (ref. 19) spectra vs. LET and measured results from the HIIS experiment on LDEF from (ref. 16).